Journal of Alloys and Compounds 509S (2011) S844–S848

Contents lists available at ScienceDirect

Journal of Alloys and Compounds

journal homepage: www.elsevier.com/locate/jallcom

Synchrotron diffraction studies and thermodynamics of hydrogen absorption–desorption processes in $La_{0.5}Ce_{0.5}Ni_4Co$

A.B. Riabov[a,b], R.V. Denys[a,b], J.P. Maehlen[a], V.A. Yartys[a,*]

[a] Institute for Energy Technology, Kjeller NO-2027, Norway
[b] Karpenko Physico-Mechanical Institute, NAS Ukraine, 5, Naukova St., Lviv 79601, Ukraine

A R T I C L E I N F O

Article history:
Received 7 October 2010
Received in revised form 9 November 2010
Accepted 16 November 2010
Available online 23 November 2010

Keywords:
Hydrogen storage
Metal hydride
Hydrogen absorption–desorption
PCT isotherms
Synchrotron X-ray diffraction
Lanthanum
Cerium
Nickel
Cobalt

A B S T R A C T

A hexagonal $CaCu_5$-type $La_{0.5}Ce_{0.5}Ni_4Co$ intermetallic alloy was studied as H storage material in as cast condition using PCT and *in situ* Synchrotron XRD studies performed between 263 and 353 K. A significant shrinking of the unit cells takes place on a substitution of La with Ce. SR XRD showed the formation of two hexagonal hydrides, a γ-trihydride $La_{0.5}Ce_{0.5}Ni_4CoH_3$, and a saturated β-hexahydride $La_{0.5}Ce_{0.5}Ni_4CoH_{\sim6}$. In addition, an α-H solid solution was experimentally observed. Hysteresis of hydrogen absorption and desorption between the flat single plateaus isotherms measured during the PCT measurements was rather small, with no indication of the formation of the thermodynamically stable γ-(La,Ce)(Ni,Co)$_5$H$_3$. The SR XRD revealed that (a) the relative abundance of the γ-hydride is higher during the desorption compared to the absorption; its relative amount reaches 50 wt.% in maximum; (b) anisotropic strains in all constituent phases during both hydrogen absorption and desorption are not developed; (c) the pressure of the formation of the γ-phase was found to be strongly temperature-dependent. The formation of large amounts of metastable γ-(La,Ce)(Ni,Co)$_5$H$_3$ hydride in quasiequilibrium experimental conditions applied during the SR XRD experiments and during reaching the thermodynamic equilibrium between the constituent phases can be responsible for the reduced hysteresis of the PCT isotherms and absence of noticeable anisotropic strains in the constituent phases.

1. Introduction

$LaNi_5$-based alloys belong to the most comprehensively studied group of hydrogen storing AB_5 intermetallics. A partial substitution of La and/or Ni by the chemically related elements (*e.g.*, Ce or Mischmetal substitution for La, and Co, Al, Mn or Sn substitutions for Ni) results in substantial changes in the physicochemistry of the hydrogenation process; a decrease of the hydride stability for the La → Ce/Mm substitution and an increase of the stability for the Ni → Co, Al, Mn or Sn substitutions are observed [1].

Akiba et al. [2] during the PCT measurements of the isotherms of hydrogen absorption and desorption and XRD studies observed that $LaNi_5$ is hydrogenated via a two-step process, forming a γ-trihydride $LaNi_5H_3$ and a hexahydride $LaNi_5H_{6.7}$ [3]. The γ-hydride was formed at elevated temperatures; in the PCT studies it was observed only in the desorption isotherms measured above 80 °C, and in the absorption isotherms above 100 °C. The XRD experiment showed that the γ phase, after being formed at higher temperatures, did not decompose on cooling down to the lower temperatures.

Joubert et al. studied the $LaNi_5$–H_2 system by *in situ* Synchrotron X-ray diffraction (SR XRD) [4]. The measurements were performed in dynamic equilibrium conditions for both charge and discharge of hydrogen gas. The γ-trihydride was observed after the first absorption during both hydrogen absorption and desorption experiments at room temperature. As four phases were observed in the studied sample at a constant interaction temperature, a disagreement with the phase equilibrium law was explained by a formation of a transient non-equilibrium γ-$LaNi_5H_3$ phase. The studies revealed that this phase is formed under quasi-isobaric hydrogen absorption–desorption in rather small quantities not exceeding 10 wt.%.

Formation of γ-trihydride in equilibrium conditions was also observed in the PCT studies of the annealed alloys where part of La was substituted by Ce and part of Ni was replaced by Co to form $La_{0.5}Ce_{0.5}Ni_{5-x}Co_x$ ($x = 0.2, 0.5, 1.0$) [5] alloys. As Co-containing $La_{0.5}Ce_{0.5}Ni_{5-x}Co_x$ are characterized by significantly reduced hysteresis of hydrogen absorption and desorption and they have reasonably high hydrogen absorption–desorption equilibrium pressures, they are excellent candidates as hydrogen absorbents for use in the thermal sorption compression of hydrogen gas. The efficiency of such compression is reduced with increased hysteresis and with sloping of the plateau pressures and is therefore strongly influenced by the mechanism and kinetics of the phase-structural

---

* Corresponding author. Tel.: +47 63 80 64 53; fax: +47 63 81 29 05.
E-mail address: volodymyr.yartys@ife.no (V.A. Yartys).

0925-8388/$ – see front matter © 2010 Elsevier B.V. All rights reserved.
doi:10.1016/j.jallcom.2010.11.116

transformations in the system during hydrogen charge and discharge. This mechanism is affected by prehistory of the sample (as cast/annealed) and by the La/Ce and Ni/Co ratios.

Present work focuses on studies of the mechanism of hydrogen absorption–desorption processes in as-cast $La_{0.5}Ce_{0.5}Ni_4Co$ alloy by the PCT measurements and *in situ* SR XRD investigations during the hydrogenation–dehydrogenation cycling at isobaric conditions.

2. Experimental

The $La_{0.5}Ce_{0.5}Ni_4Co$ alloy was prepared by arc melting of the high purity constituent elements, La, Ce, Ni and Co (all ≥99.9%), in a protective atmosphere of argon gas (purity 99.999%). The alloy sample was remelted two times to ensure its homogeneity. Its properties were studied in as cast condition. XRD measurements showed formation of a single phase hexagonal $CaCu_5$-type intermetallic compound ($a = 4.9437(3)$ Å, $c = 3.9846(2)$ Å; $V = 84.34(1)$ Å^3). As expected, the unit cell parameters have intermediate values between those for $LaNi_4Co$ ($a = 5.031$ Å and $c = 3.984$ Å) [6] and $CeNi_4Co$ ($a = 4.895$ Å and $c = 3.998$ Å) [7] compounds.

To measure the hydrogen absorption and desorption isotherms, ~1 g of the $La_{0.5}Ce_{0.5}Ni_4Co$ alloy was placed into a stainless steel reactor and connected to a Sieverts' type apparatus. First hydrogenation experiment was started without a preliminary high-temperature activation of the alloy; the sample was only degassed at room temperature in a vacuum of $\sim 10^{-3}$ mbar for 30 min. Initial hydrogenation was performed at 293 K and 70 bar H_2 pressure. Maximum hydrogenation capacity of 6.7 at. H/f.u. was reached in 30 min, after an incubation period of ~15 min. Synthesized sample was dehydrogenated in dynamic vacuum at 363 K and hydrogenated again at 293 K and 70 bar H_2. During the second and following hydrogenation cycles, full hydrogen saturation was achieved very rapidly, within less than 30 s. Absorption and desorption isotherms were then measured at temperatures 273, 313 and 353 K in the pressure range from 0.01 to 100 bar.

For the *in situ* SR XRD measurements the alloy powder was loaded into an open-ended 0.3 mm quartz capillary, which was then placed inside a sealed 0.5 mm capillary connected to the Sieverts' type gas system via a modified SS-Tee joint attached to a goniometer head. Heating and cooling of the sample were performed by a programmable cryostream system allowing desired heating/cooling rates at temperatures 77–500 K. First, the $La_{0.5}Ce_{0.5}Ni_4Co$ was activated by subjecting it to a pressure of 50 bar H_2 at 380 K to ensure the formation of a single-phase α-solid solution of hydrogen. Then, the first hydrogenation was initiated by cooling the sample to 263 K. The diffraction data were collected at constant hydrogen pressures of 9, 14 or 25 bar H_2, during heating/cooling of the sample at different constant ramp rates of 1, 2 or 4 K/min. The temperature was increased to 353 K for hydrogen desorption and decreased to 263 K for H_2 absorption.

The SR XRD data were collected at the Beam Line 01A, Swiss-Norwegian Beam Lines, ESRF, Grenoble, using a MAR2300 image plate detector. The wavelength was $\lambda = 0.7350$ Å; the measurements covered an angle interval 2θ from 3.12° to 40.92°. Each pattern was collected during 20 s. The intervals between the consecutive scans were ~1.5 min, as they included the time of the reading of the data from the image plate. The collected data were integrated using the software Fit2D. A LaB_6 standard was used to determine the instrumental constants.

The collected SR XRD data were evaluated using the Rietveld profile refinement method with the GSAS software package [8]. Since the XRD data do not allow to differentiate Ni and Co, during the refinements of the data for $La_{0.5}Ce_{0.5}Ni_4Co$ we have adopted a model of preferred occupancy by Co of the 3g site, as suggested in [6] for $LaNi_4Co$: 1.75 Ni + 0.25 Co in 2*b* (1/3, 2/3, 0); 2.25 Ni + 0.75 Co in 3*g* (1/2, 0, 1/2).

3. Results and discussion

3.1. PCT diagrams

Fig. 1 presents results of the PCT measurements of hydrogen absorption and desorption isotherms in the $La_{0.5}Ce_{0.5}Ni_4Co–H_2$ system and corresponding van't Hoff plots. The data were collected at 273, 313 and 353 K. The measured points are shown by symbols, whereas the calculated isotherms are modelled according to Lototsky et al. [9]. The isotherms show a single-plateau behaviour with small hysteresis between the absorption and desorption pressures and modest slopes. The measured maximum hydrogen storage capacity, 6.7 at. H/f.u., equals to the highest observed for the AB_5 series capacity, *e.g.* $LaNi_5H_{6.7}$ [3]. Evaluation of the van't Hoff plots (Fig. 1(b)) provided the following thermodynamic parameters of the metal–hydrogen interactions for the $La_{0.5}Ce_{0.5}Ni_4Co–H_2$ system: $\Delta H_{abs} = -27.1 \pm 0.8$ kJ/mol H_2; $\Delta S_{abs} = -111.1 \pm 2.5$ J/(mol K); $\Delta H_{des} = 27.4 \pm 1.1$ kJ/mol H_2; $\Delta S_{des} = 110.8 \pm 4.1$ J/(mol K). A summary of the collected thermodynamic data is summarized in Table 1.

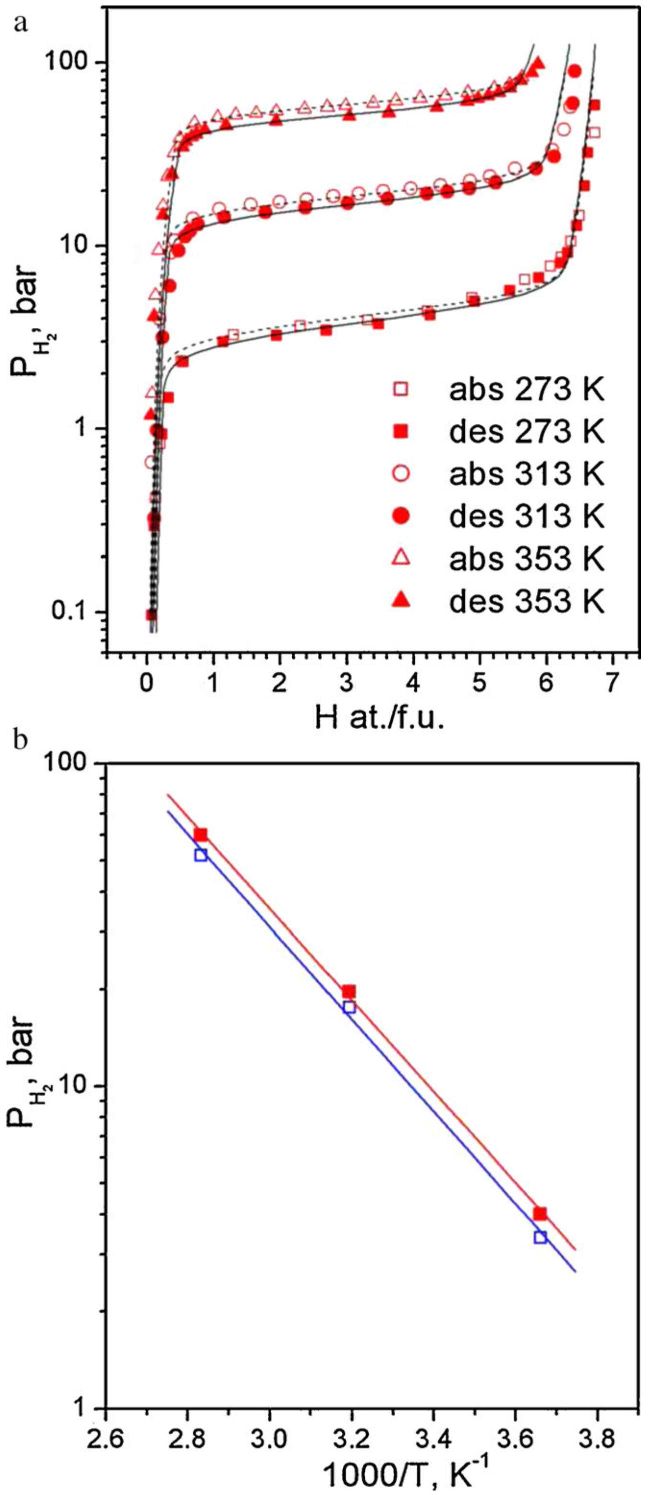

Fig. 1. Pressure-composition isotherms (a) and van't Hoff plots (b) for the $La_{0.5}Ce_{0.5}Ni_4Co–H_2$ system.

Ce replacement for La significantly decreases hysteresis, from 1.7 kJ/mol H_2 for $CeNi_4Co–H_2$ system [7] to 0.3–0.4 kJ/mol H_2 for the $La_{0.5}Ce_{0.5}Ni_4Co–H_2$ system. A possible reason for that will be discussed later in the paper.

Table 1
Data of the PCT characterisation of the $La_{0.5}Ce_{0.5}Ni_4Co–H_2$ system.

Temperature	Absorption pressure	Desorption pressure	C_{max} (H/f.u.)	P_{max} (bar)	Hysteresis RTln(P_{abs}/P_{des}) (kJ/mol H_2)
273	4.0	3.4	6.73(5)	58	0.38
293			6.67(5)	66	
313	19.6	17.6	6.44(5)	90	0.28
353	59.7	51.8	5.87(4)	98	0.41

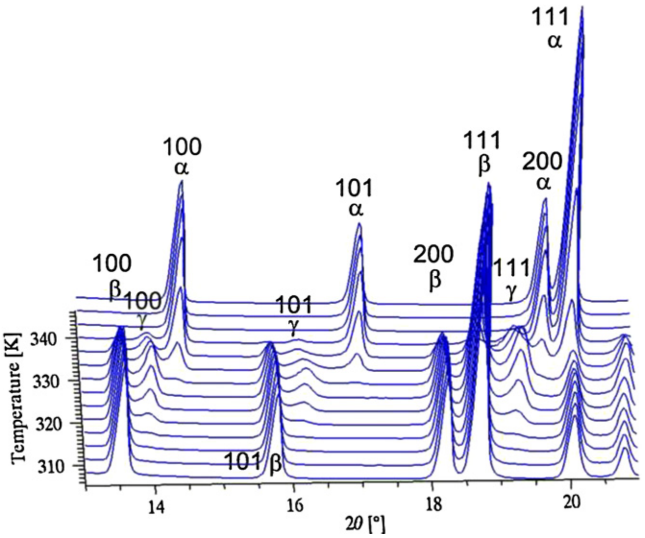

Fig. 2. Temperature evolution of the *in situ* SR XRD pattern during hydrogen desorption from the β-$La_{0.5}Ce_{0.5}Ni_4CoH_{\sim 6}$ hydride. Miller indices of the diffraction peaks for three constituent phases are shown.

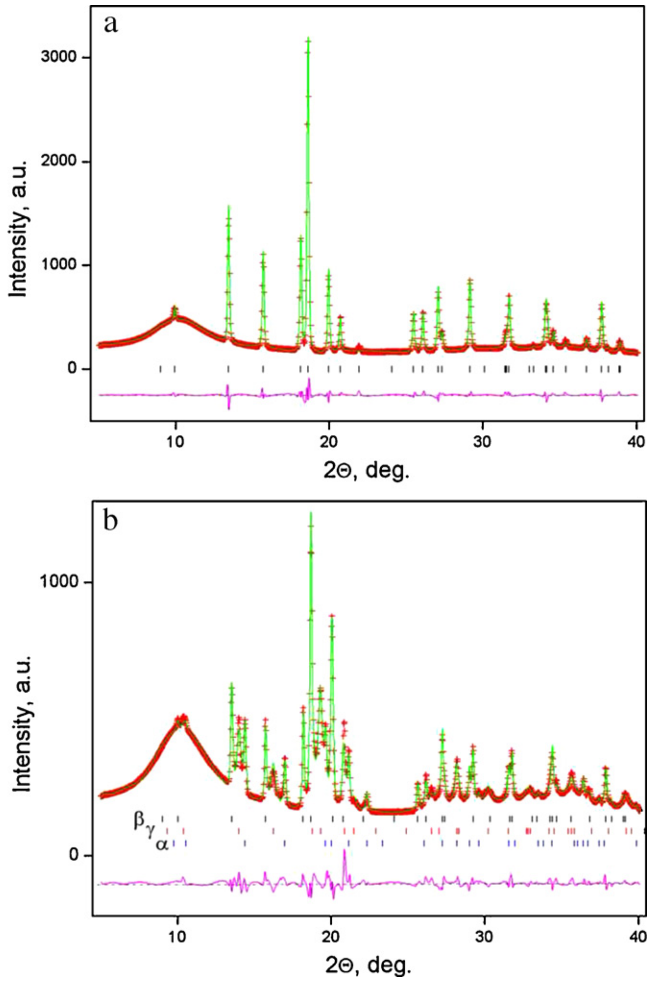

Fig. 3. Measured (+), calculated (line) and difference (lower line) plots of Rietveld refinements of the SR XRD data for (a) single-phase β-$La_{0.5}Ce_{0.5}Ni_4CoH_{\sim 6}$ (25 bar H_2, 283 K) with inset showing the changes of the unit cell volume for γ-hydride during the H_2 absorption and desorption, and (b) mixture of three hydrides (β-hydride 27.9 wt.%, γ-hydride 51.3 wt.%, α-hydride 20.8 wt.%; data collected at 25 bar H_2, 331 K,).

3.2. *In situ* Synchrotron X-Ray diffraction studies

Although the PCT measurements indicated the presence of only two phases, an α-H solid solution $La_{0.5}Ce_{0.5}Ni_4CoH_{\sim 0.5}$ and a saturated β-hexahydride $La_{0.5}Ce_{0.5}Ni_4CoH_{\sim 6}$ ($\Delta V/V = 24.5\%$; lattice expansion is similar along [0 0 1], 6.0%, and in the basal plane, 8.8.%), the *in situ* SR-XRD hydrogen absorption and desorption experiments performed at constant H_2 pressures revealed the formation of an intermediate γ-trihydride $La_{0.5}Ce_{0.5}Ni_4CoH_{\sim 3}$ ($\Delta V/V = 12.9\%$; lattice expansion mainly in the basal plane, 5.3%, and is much less pronounced along [0 0 1], 1.9%).

Fig. 2 presents the evolution of the SR XRD pattern during decomposition of the β-hexahydride. The pattern was collected at a constant H_2 pressure of 25 bar H_2 using a heating rate of 2 K/min in the temperature interval from 312 to 352 K. Fig. 3 shows two representative Rietveld refinement plots. A pattern from a single phase β-hydride is given in Fig. 3(a) (data collected at 283 K), while Fig. 3(b) shows the pattern collected during a desorption experiment performed at 311 K. The latter experiment shows a formation of a mixture of three hydrogen-containing phases, β- and γ-hydrides and α-solid solution of H in the $La_{0.5}Ce_{0.5}Ni_4Co$. Crystallographic data for the observed phases measured at 293 K are provided in Table 2.

We note that the formation of the γ-hydride during hydrogen absorption and desorption experiments does not agree with the single-plateau behaviour observed in the PCT measurements of the studied system and violates the Gibb's phase law. The reason for such a disagreement is different conditions of these two experiments; thermodynamically equilibrium conditions during the PCT measurements and, in contrast, non-equilibrium, dynamic processes of hydrogen charge and discharge during the *in situ* SR XRD measurements.

Table 2
Crystallographic data for $La_{0.5}Ce_{0.5}Ni_4Co$ and its hydrides at 293 K.

Composition	a (Å)	c (Å)	V (Å$^{3)}$	$\Delta V/V$ (%)
$La_{0.5}Ce_{0.5}Ni_4Co$	4.9437(3)	3.9846(2)	84.34(1)	
α-$La_{0.5}Ce_{0.5}Ni_4CoH_{\sim 0.5}$	4.9724(2)	3.9990(2)	85.626(8)	1.5
γ-$La_{0.5}Ce_{0.5}Ni_4CoH_{\sim 3}$	5.2044(7)	4.061(1)	95.26(3)	12.9
β-$La_{0.5}Ce_{0.5}Ni_4CoH_{\sim 6}$	5.3793(4)	4.2250(4)	105.88(2)	25.5

Analysis of the peak shapes of the pattern shown in Figs. 2 and 3 does not provide any indication of a noticeable anisotropic peak broadening. This contrasts to the hydrogenation behaviour reported earlier for the hydrides of $LaNi_5$ [10] and $CeNi_5$ [11] and attributed to the appearance of anisotropic lattice strains in the samples caused by the formation and decomposition of the hydride phases. These strains appeared after the first hydrogenation and were observed during further absorption–desorption cycling. Absence of the strains in the system studied in the present work is presumably caused by the formation of substantial amounts of γ-phase, both during hydrogenation and dehydrogenation processes (30–50 wt.% compared to the 10–15 wt.% in [4]). Because of intermediate values of the *a* and *c* lattice parameters for the γ-hydride between the α-solid solution and the β-hydride, its presence reduces/minimizes stresses in the material, thus eliminating the reasons causing the anisotropic peak broadening. Larger amount of the formed γ-hydride assists in separating the α-solution and the β-hydride and in realising the "stress-free" reaction interface.

This feature of the studied system is likely to be also responsible for a rather small hysteresis observed in the PCT measurements between the hydrogenation and dehydrogenation. Although the PCT isotherms do not show any indication of the existence of the thermodynamically stable γ-hydride, its formation in the dynamic conditions of hydrogen transfer through the sample to form the β-hydride or during decomposition of the β-hydride to form the α-solid solution, while reaching equilibrium hydrogen concentrations, may well happen.

Fig. 4(a)–(c) presents changes in the phase-structural composition of the samples during hydrogen desorption and absorption experiments, proceeding during the heating or cooling of the samples with a rate of 2 K/min at constant H_2 pressures of 9, 14 or 25 bar. The data collected at variable heating/cooling rates indicate similar features for all studied systems. The γ-hydride was found to be formed during all desorption and absorption experiments. However, its existence is limited to a rather narrow temperature range of ~20–30 K. During the desorption process, at a certain turnover temperature, β-hydride starts to transform into the γ-hydride; *vice versa*, during hydrogen absorption by the alloy during cooling of the system, below the same turnover temperature the $\alpha \rightarrow \gamma$ transformation proceeds. Independently of the applied pressure, the amount of the γ-hydride formed during the desorption is about twice as high as its maximum content in the system during the hydrogen absorption (>50 wt.% and <30 wt.%, respectively).

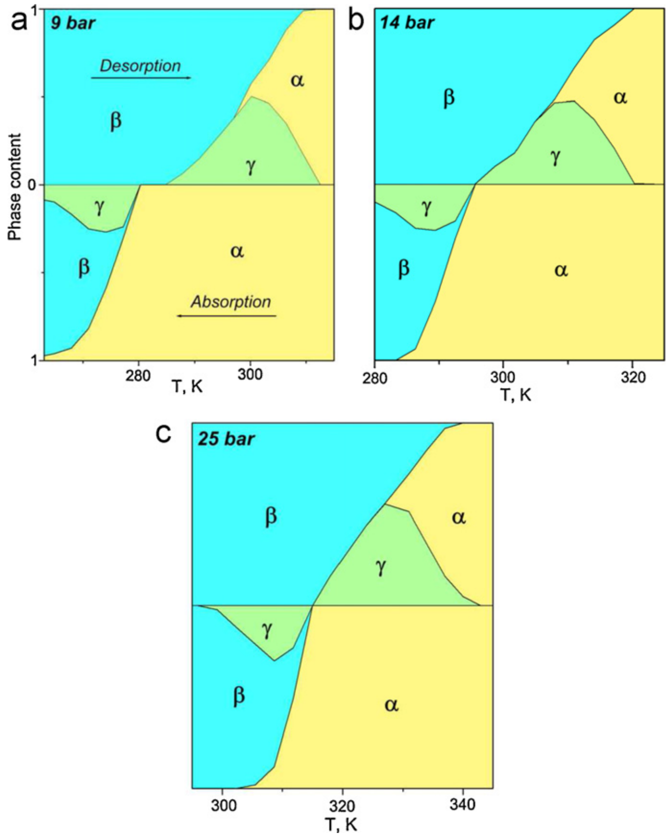

Fig. 4. Phase-structural composition of the $La_{0.5}Ce_{0.5}Ni_4Co–H_2$ system from the refinements of the SR XRD data during isobaric desorption (upper part; heating) and absorption (lower part, cooling) with a heating/cooling rate of 2 K/min under isobaric conditions, 9 bar H_2 (a), 14 bar H_2 (b) or 25 bar H_2 (c).

The decomposition of the hydride and the reverse hydrogenation processes seem to follow different reaction pathways. During the hydrogen desorption, the $\beta \rightarrow \gamma$ transformation takes place first and then, after the formed amount of γ-hydride reaches its maximum content, the transformations in the formed three-phase $\alpha + \beta + \gamma$ system proceed via two parallel mechanisms, $\beta \rightarrow \alpha$ and $\gamma \rightarrow \alpha$, finally yielding a single-phase α-solid solution. On cooling the sample, after reaching a turnover temperature, α-solid solution is hydrogenated to form in parallel two hydrides, γ and β, via the $\alpha \rightarrow \gamma$ and $\alpha \rightarrow \beta$ transformations.

From the refinements of the *in situ* diffraction pattern, we conclude that all three hydrogen-containing phases have certain homogeneity ranges. Indeed, following the temperature increase from 263 to 344 K, the unit cell of the β-$La_{0.5}Ce_{0.5}Ni_4CoH_{\sim 6}$ undergoes a contraction by 1.4%. For the γ-hydride, a similar but much stronger effect is observed, with a very significant shrinking of the volume by 2.6% proceeding in a narrow temperature interval between 288 and 313 K. Even for the α-solid solution, quite a significant volume change of −1.4% on heating the sample between 300 and 344 K was observed, indicating rather significant hydrogen solubility in it; these decrease at higher temperatures. We note that the relative effect from the changes in hydrogen content is probably even higher, as the volume shrinking on heating is in part compensated by the thermal expansion of the metal matrix. Continuous change of the unit cell parameters of the constituent phases with hydrogen content, also helps in reducing interfacial stresses between the components of the three-phase hydride system, thus further decreasing and eliminating the appearance of the anisotropic stresses in the metal matrices.

Evaluation of the SR XRD allowed to calculate the temperature dependences of hydrogen content in the systems during the absorption–desorption processes in the isobaric condition (Fig. 5).

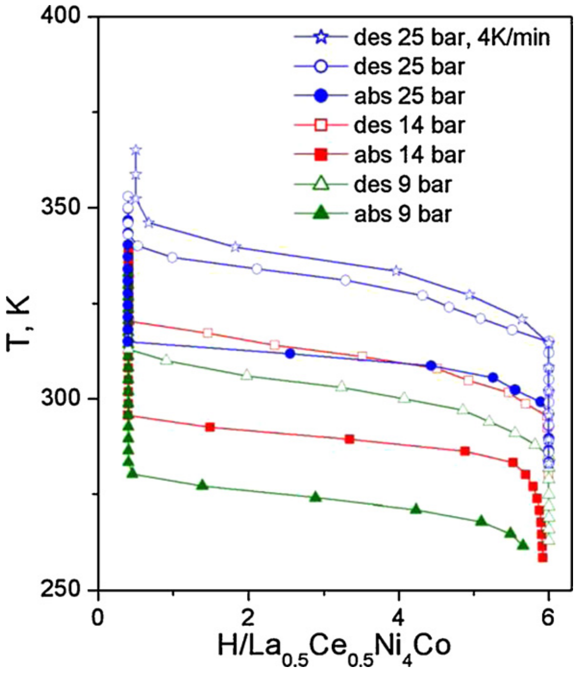

Fig. 5. Calculated isobars of hydrogen desorption and absorption built on the basis of the refined SR XRD data.

The “isobars” are built assuming that H content equals to 0.5, 3 and 6 at. H/$La_{0.5}Ce_{0.5}Ni_4Co$ for the α-, γ- and β-phases, respectively, during the heating/cooling experiments with a rate of 2 K/min. As can be seen from Fig. 5, the temperatures of the mid-plateaux on the isobars continuously increase, from 273 to 310 K for the absorption and from 303 to 330 K for the desorption processes, following the increase in hydrogen pressures. The observed 20–30 K hysteresis between the hydrogen absorption and desorption well agrees with an assumption of a kinetic control of the rate of the transformation processes. At the highest applied heating rate of 4 K/min the desorption isobar is shifted towards the higher plateau temperatures, further supporting a suggestion of the kinetic control over the rate of the process.

As can be seen from Fig. 4, the hydrogenation of the γ-hydride to produce β-hydride is a much faster process as compared to the desorption of hydrogen from the γ-hydride to yield the H α-solid solution. Indeed, maximum observed content of γ-hydride is smaller, while the temperature range and duration of its existence are narrower for the hydrogenation processes where the $\alpha \rightarrow \gamma \rightarrow \beta$ transformations take place.

4. Conclusions

As cast $La_{0.5}Ce_{0.5}Ni_4Co$ alloy represents a new example of the AB_5-hydrogen system where α-solid solution and two hydrides, β-$La_{0.5}Ce_{0.5}Ni_4CoH_6$ and γ-$La_{0.5}Ce_{0.5}Ni_4CoH_3$, are simultaneously observed at certain pressure–temperature–time non-equilibrium dynamic conditions of hydrogen charge or discharge, as revealed by the *in situ* SR XRD studies. This finding formally conflicts with the observed single-plateau shape of the isotherms of hydrogen absorption and desorption and the Gibbs’ phase rule. Earlier such behaviour was reported for the $LaNi_5$ intermetallic. However, the SR XRD data for the $La_{0.5}Ce_{0.5}Ni_4Co–H_2$ does not show any noticeable anisotropic broadening of the diffraction peaks, in contrast to the $LaNi_5–H_2$ system, where such a broadening took place and $\alpha + \beta + \gamma$ samples were formed at the dynamic non-equilibrium conditions [4].

Quite typically for the $AB_5–H_2$ systems, the rates of the hydride formation are higher compared to the hydride decomposition. The *in situ* SR XRD revealed that under applied isobaric conditions, the γ-hydride is formed in larger quantities during the hydrogen desorption compared to the H_2 absorption. This phase exists in a rather narrow temperature interval of 20–30 K. The larger amount of γ-hydride formed during the desorption indicates that in a competition between the two reaction pathways, $\beta \rightarrow \alpha$ or $\beta \rightarrow \gamma \rightarrow \alpha$, the latter seems to be the preferable one; in contrast, during the hydrogen absorption the transformation proceeds mostly by the direct $\alpha \rightarrow \beta$ reaction rather than by a step-by-step $\alpha \rightarrow \gamma \rightarrow \beta$ process.

Replacement of Ni by Co and Ce by La dramatically reduced hysteresis between the H absorption and desorption in the Ce-containing AB_5 hydrides. The observed hysteresis values are much smaller than those for the $CeNi_4Co$. The reasons for the reduced hysteresis and absence of anisotropic strain broadening for the as cast $La_{0.5}Ce_{0.5}Ni_4Co$ is in the formation of the “stress-free” reaction interface, where α-solution and the β-hydride are separated by the formed γ-hydride. As the γ-hydride has intermediate values of the *a* and *c* lattice parameters between the α-solid solution and the β-hydride, its presence reduces or even eliminates the reasons for the two mentioned phenomena.

A significant difference observed between the as cast and annealed $La_{0.5}Ce_{0.5}Ni_4Co$ alloy could be caused by different ordering of Co and Ni between the 2b and 3g sites. This feature has not been studied for the as cast alloy and is planned to be investigated by neutron powder diffraction.

Acknowledgements

This work has received a support from the Norwegian Research Council.

A skillful assistance from the staff of the Swiss-Norwegian Beam Lines during the experimental studies at ESRF is gratefully acknowledged.

Dr. Mykhaylo Lototskyy (University of the Western Cape, South Africa) is sincerely thanked for the assistance in the evaluation of the experimental data.

References

[1] T. Sakai, M. Matsuoka, C. Iwakura, in: K.A. Gschneider Jr., L. Eyring (Eds.), Handbook on the Physics and Chemistry of Rare Earths, vol. 21, Elsevier, Amsterdam, 1995, p. 133 (Chapter 142).
[2] E. Akiba, K. Nomura, S. Ono, J. Less-Common Met. 129 (1987) 159–164.
[3] C. Lartigue, A. Percheron-Guegan, J.C. Achard, J.L. Soubeyroux, J. Less-Common Met. 113 (1985) 127–148.
[4] J.-M. Joubert, R. Černý, M. Latroche, A. Percheron-Guégan, B. Schmitt, Acta Mater. 54 (2006) 713–719.
[5] D. Dayan, M.H. Mintz, M.P. Dariel, J. Less-Common Met. 73 (1980) 15–24.
[6] M. Latroche, J. Rodriguez-Carvajal, A. Percheron-Guégan, F. Bourée-Vigneron, J. Alloys Compd. 218 (1995) 64–72.
[7] S.N. Klyamkin, N.S. Zakharkina, A.A. Tsikhotskaya, J. Alloys Compd. 398 (2005) 145–151.
[8] A.C. Larson, R.B. von Dreele, General Structure Analysis System, LANL, 1994.
[9] M.V. Lototsky, V.A. Yartys, V.S. Marinin, N.M. Lototsky, J. Alloys Compd. 356–357 (2003) 27–31.
[10] R. Černý, J.-M. Joubert, M. Latroche, A. Percheron-Guégan, K. Yvon, J. Appl. Cryst. 33 (2000) 997–1005.
[11] V.A. Yartys, R.V. Denys, J.P. Maehlen, C.J. Webb, E. MacA. Gray, T. Blach, A.A. Poletaev, J.K. Solberg, O. Isnard. In In-Situ and Operando Probing of Energy Materials at Multiscale Down to Single Atomic Column—The Power of X-Rays, Neutrons and Electron Microscopy, in: C.M. Wang, N. de Jonge, R.E. Dunin-Borkowski, A. Braun, J-H. Guo, H. Schober, R.E. Winans (Eds.) (Mater. Res. Soc. Symp. Proc. Volume 1262, Warrendale, PA, 2010), Paper #: 1262-W04-01. DOI: 10.1557/PROC-1262-W04-01. ISBN: 978-1-60511-239-8. Proceedings of the 2010 MRS Spring Meeting. 5–9 April 2010. San Francisco, USA.